REPORT DOCUMENTATION PAGE

Form Approved
OMB No. 0704-0188

1. AGENCY USE ONLY (Leave blank)	2. REPORT DATE	3. REPORT TYPE AND DATES COVERED
	May 1995	Final Technical Report 9/30/93-3/29/95

4. TITLE AND SUBTITLE

Large Eddy Simulation of Turbulent Flow Over an Airfoil

5. FUNDING NUMBERS

F49620-93-1-0629

6. AUTHOR(S)

Professor Parviz Moin

7. PERFORMING ORGANIZATION NAME(S) AND ADDRESS(ES)

Stanford University
Mechanical Engineering
Thermosciences Division
Stanford, CA 94305-3030

AFOSR-TR-95
0511

9. SPONSORING/MONITORING AGENCY NAME(S) AND ADDRESS(ES)

Air Force Office of Scientific Research
Dr. Leonidas Sakell
110 Duncan Avenue, Suite B115
Bolling AFB, DC 20332-0001

NA

10. SPONSORING/MONITORING AGENCY REPORT NUMBER

F49620-93-1-0629

11. SUPPLEMENTARY NOTES

12a. DISTRIBUTION/AVAILABILITY STATEMENT

Approved for public release.
Distribution is unlimited.

12b. DISTRIBUTION CODE

13. ABSTRACT (Maximum 200 words)

The turbulent flow over a NACA 4412 airfoil at angle of incidence corresponding to maximum lift (12 degree) has been computed via large-eddy simulation. Two different numerical approaches, one based on a conventional structured mesh and one with a more economical unstructured mesh, have been employed. Results from both simulations differ considerably from each other and from the available experimental data. Differences are found with respect to occurrence of transition near the suction peak and with respect to the amount of backflow (incipient separation) near the trailing edge. The unstructured mesh code predicts rapid boundary layer growth and separation near the trailing edge, whereas the flow remains attached in the structured mesh simulation. It was concluded that a better matching of the transition mechanism (boundary layer tripping) which was employed in the experiments is paramount for an accurate simulation of this flow and for convergence of solutions from the two codes.

14. SUBJECT TERMS

large eddy simulation, dynamic model, incipient separation

15. NUMBER OF PAGES

16

16. PRICE CODE

17. SECURITY CLASSIFICATION OF REPORT	18. SECURITY CLASSIFICATION OF THIS PAGE	19. SECURITY CLASSIFICATION OF ABSTRACT	20. LIMITATION OF ABSTRACT
unclassified	unclassified	unclassified	

Final Technical Report for:

LARGE EDDY SIMULATION OF TURBULENT FLOW OVER AN AIRFOIL

Project #F49620-93-1-0629

Submitted by:

Parviz Moin
Stanford University
Mechanical Engineering, Thermosciences Division
Stanford, CA 94305-3030
Phone: (415) 723-9713

Submitted to:

Leonidas Sakell
Air Force Office of Scientific Research
Bolling Air Force Base
Washington, DC 20332-0001
Phone: (202) 767-4935

For the Period:

September 30, 1993 through March 29, 1995

1 Background

The technique of large-eddy simulation (LES) has been successfully applied to a variety of flows, ranging from wall-bounded shear flows to flows with separation from sharp corners (backstep, cubic obstacles) or smooth surfaces (cylinder). Also, transition to turbulence has been successfully predicted by LES. The discovery and subsequent development of the dynamic procedure for modeling subgrid-scale stresses by the CTR group (Germano *et al.* 1991, Moin *et al.* 1991, Ghosal *et al.* 1995) has created a rather universal simulation technique with the potential to accurately predict flows of aeronautical interest. The diversity of flow characteristics encountered in a typical flow over an airfoil near maxmimum lift taxes the presently available statistical turbulence models. An example which demonstrates some weakness of current RANS predictions will be given below.

The main obstacles for application of LES to a wider range of flows were the lack of reliable subgrid-scale (SGS) models, the need for accurate numerical methods, and the high computational costs. As mentioned before, the introduction of the dynamic subgrid-scale model has removed the arbitrariness which was inherent in earlier SGS-models. Most LES up to now were done with either spectral methods - which are highly accurate but not easily extendable to generalized coordinates - or finite-difference based methods on structured meshes. The computational costs of LES are largely dominated by the need of resolving at least part of the boundary-layer turbulence on the airfoil surface. This makes structured mesh codes unattractive because the fine near-wall resolution has to be carried through the whole domain and even in the freestream. Conversely, finite element (FE) methods on unstructured meshes provide the opportunity to cluster grid-points in all three dimensions at locations which are dictated by the flow physics. Substantial savings in terms of grid-points can be realized through this approach compared to a structured mesh. However, very few direct (DNS) or large-eddy simulations of turbulent flows using FE-methods have been attempted. We therefore felt that it would be wise to attack this problem with two numerical methods in parallel. An existing finite difference code that had been used for both DNS and LES has been adapted to allow for simulation of flow over an airfoil on a C-mesh. In parallel, a FE-code for LES has been developed which runs very efficiently on parallel machines.

The flow configuration chosen is a NACA 4412 airfoil at maximum lift. The corresponding angle of attack was determined independently by Wadcock (1987) and Hastings & Williams (1984, 1987) to be close to 12°. The chord Reynolds number $U_\infty c/\nu$ was similar in both experiments, 1.64×10^6 in Wadcock (1987) and 4.2×10^6 in Hastings (1984). In his more recent work, Wadcock found that the pressure distribution of earlier measurements taken at CALTECH at $\alpha = 13.57°$ (Coles & Wadcock, 1979) was identical to the one obtained later in the NASA facility at $\alpha = 12°$ and obtained by Hastings (1984) at $\alpha = 12.15°$. From this he concluded that the Coles & Wadcock (1979) measurements corresponded to an effective angle close to 12° rather than to the nominal angle of $\alpha = 13.57°$. Wadcock (1987)also mentions that a change of inclination angle by 1° moves the separation point back or forwards by about 15% of chord.

Rogers *et al.* (1992) and Durbin (1993) computed this flow using RANS-based models. In both cases, α was set to 14°. Results, however, were compared to measurements from 12°.

Both CFD-solutions predict about the right amount of backflow in the last 20% of chord. Personal communication with the above authors confirms that both RANS-models underpredict separation for the correct angle of incidence $\alpha = 12°$.

2 Objectives

The work which is described in this report was carried out with the following goals:

1. Development of an incompressible, structured mesh, finite difference LES-code with the dynamic SGS-model for simulation of flow over an airfoil on a C-mesh.
2. Development of an unstructured mesh, finite element method for simulation of turbulence. This code solves the compressible Navier-Stokes equations, uses the dynamic model and runs on parallel computers.
3. Validation of both methods by computing vortex shedding behind a cylinder.
4. Simulation of flow around an airfoil near maximum lift angle of incidence and comparison with experimental data from Coles & Wadcock (1978), Hastings & Williams (1984) and Wadcock (1987).
5. Evaluation of resolution requirements and cost for each numerical method.
6. Assessment of the role of the subgrid-scale model.

3 Accomplishments

We describe the two numerical approaches before we present simulation results and compare them to measurements.

3.1 Finite difference method on structured mesh

The incompressible Navier-Stokes equations are solved with a second-order finite difference method in generalized coordinates in a spanwise periodic domain. The method is described in more detail in Choi *et al.* (1993). The staggered configuration of velocity components and pressure guarantees conservation of mass, momentum and kinetic energy on equispaced meshes. Only mass is exactly conserved in the formulation in generalized coordinates. On the C-shaped domain we specify freestream velocities at the outer boundary, no-slip at the wall and use a convective boundary condition at the outflow. The outer boundary is about three chord-lengths away from the surface. Preliminary RANS-computations were performed to confirm that the flow near the body was not influenced by the location of the outer domain boundary. The code was validated by computing the laminar vortex shedding behind a cylinder (Choi, 1993).

Centered difference schemes suffer from the emergence of grid-to-grid oscillations (2-Δ-waves) when used for high Reynolds number simulations because they lack numerical dissipation. Usually, the viscosity provided by the subgrid-scale model is sufficient to dampen these grid-to-grid oscillations. However, mesh stretching can badly affect the properties of a scheme. As shown by Cain & Bush (1994), waves propagating into an increasingly coarse (fine) mesh are amplified (dampened) in a centered scheme. In our simulation we found that strong 2-Δ-waves emerged near the nose and near the trailing edge where the mesh was stretched. Despite a great effort in designing a smooth variation in spacing we had to resort to an *ad hoc* modification of the numerical scheme. For a very limited spatial extent (less than 2% of the chord) we applied a 1:2:1-filter in the streamwise and spanwise direction which efficiently eliminates all 2-Δ-waves. Justification for this procedure comes from the fact that the flow near the nose is laminar and filtering on a scale of the grid resolution does not affect the flow physics. Additionally, the boundary layer in the experiments was tripped at a location around $x/c = 0.02$, thereby fixing the region of laminar-turbulent transition. We find that the flow spontaneously transitions as soon as the filter ends. In this sense, we control the location of transition by setting the streamwise extent of the region where the solution is filtered. No attempt was made to damp 2-Δ-waves in the trailing edge region where the flow is fully turbulent. Any filtering there would probably affect the flow physics.

The dynamic subgrid-scale model has been implemented in a version which is suitable for spanwise periodic flows. The model coefficient is obtained as a spanwise averaged value. The implementation has been verified by comparison with an independent code for incompressible flow on a staggered, curvilinear mesh. The semi-implicit time advancement (third-order Runge-Kutta in combination with Crank-Nicholson) with a CFL limit of 1.5 results in an average timestep of $2 \times 10^{-4} c/U_\infty$. About 80 CPU-seconds on a Cray-C90 are needed to advance the solution over one timestep on a mesh of $640 \times 80 \times 48 = 2.5 \times 10^6$ cells. Therefore, simulation of one time unit c/U_∞ requires 90 CPU-hours.

3.2 Finite element method on unstructured mesh

The compressible Navier-Stokes equations are solved on an unstructured grid via a Galerkin/least-squares stabilized finite element method based on the work of Jansen *et al.* (1993). The stabilization is not accomplished by upwinding rather it is achieved by forming a square of the integrated residual and minimizing it simultaneously with the original Galerkin residual. Being residual based, any order method can be obtained by the proper choice of the interpolating function space. The current implementation uses linear interpolation and is globally second order accurate in space. Local error analysis of this method exhibits higher accuracy. The time integration is performed implicitly using the Crank-Nicholson method on all terms. The SGS model used is a variant of the dynamic model. New filters have been developed for the unstructured grid and have been shown to be both effective and efficient.

The current calculations use 0.5×10^6 points (3.0×10^6 tetrahedra) to discretize a domain extending 50 chord lengths away from the airfoil. The calculation requires about 10 seconds per time step on a 512 node CM5 and about 8.0 gigabytes of core memory. This translates to approximately 25 hours per time unit c/U_∞.

3.3 Mesh generation

The design of an adequate mesh involves several aspects. Firstly, the most energetic eddies of the boundary layer have to be resolved. For wall-bounded shear flows with zero-pressure gradient a more or less general criterion exists for grid-spacing in terms of wall units. However, little is known about the minimum requirements for boundary layers which are close to separation. Grid-spacing in terms of wall units probably becomes less relevant in this case. For the structured mesh simulation, about half of the 640 streamwise points were distributed over the upper surface which guaranteed that the streamwise spacing was between 1/3 and 1/5 of the local boundary layer thickness except for the nose section, see Table 1. The streamwise spacing varies considerably along the surface due to the boundary layer growth. Near the trailing edge, the grid was refined in x in order to adequatly resolve the merging of the two shear layers. No attempt was made to resolve the turbulence on the lower side of the airfoil. Spacings in terms of wall units are given in Table 1. Over a spanwise domain-size of $0.05c$ we distributed 48 points. Analysis of spanwise two-point-correlations reveals that the spanwise extent of the domain is adequate for at least two thirds of the airfoil chord. With the available resources we could not afford a simulation on a wider domain. In the wall-normal direction we used a

x/c	δ_{99}	Δx	Δx^+	Δz^+	NYBL	$\Delta x/\Delta z$
0.1	0.004	0.0031	405	137	24	2.96
0.2	0.006	0.0033	378	118	29	3.2
0.4	0.016	0.0033	274	86	33	3.2
0.6	0.030	0.0050	235	49	34	4.8
0.8	0.060	0.0088	110	13	39	8.5

Table 1: Spacing along upper surface for airfoil LES on a structured mesh. Lengths are non-dimensionalized with chordlength c. Wall units are computed using Wadcock's (1987) skinfriction measurements. NYBL denotes the number of wall-normal points inside of the boundary layer.

hyperbolic mesh generator (Chan, 1993) to distribute 80 layers of mesh cells. The first line away from the wall was at about $y^+ = 1$ and over most of the surface there were between 20 and 30 points inside of the boundary layer.

The unstructured grid method offers the opportunity to provide fine resolution only where necessary. The grid can be coarsened where resolution is less critical. The power of this approach will only be fully understood after careful studies. The preliminary work presented in this report used a grid similar to the structured grid (described above) at the wall. The spanwise resolution was then improved in the first half of the chord and coarsened in the second half of the chord in anticipation of the growth of the energy containing eddies with boundary layer thickness. Table 2 quantifies the spacing for the unstructured grid at the wall. The mesh was then generated in layers moving away from the wall where the spanwise resolution was gradually coarsened. Outside of the boundary layer the grid was coarsened to only two points

in the spanwise direction since the flow in this region has no spanwise variation. Streamwise resolution was also coarsened outside of the boundary layer. This coarsening results in a factor of five reduction in the number of points. A new mesh generator was developed to accomplish this variation in a manner smooth enough to meet the accuracy requirements of LES. We have also investigated coarsening the grid in the streamwise direction while still in the boundary layer. Preliminary results suggest that this Reynolds number is probably too low to use this approach though it did result in another factor of two reduction in the number of grid points. At higher Reynolds numbers this capability will be more important.

x/c	δ_{99}	Δx	Δx^+	Δz^+	NYBL	$\Delta x/\Delta z$
0.1	0.004	0.0026	348	87	26	3.9
0.2	0.006	0.0030	342	84	30	4.1
0.4	0.016	0.0041	343	83	38	4.1
0.6	0.030	0.0066	304	76	40	3.9
0.8	0.060	0.0120	160	36	43	4.3

Table 2: Spacing along upper surface for airfoil LES on an unstructured mesh. Same notations as in Table 1.

3.4 Simulation results

3.4.1 Time series

Figure 1 shows the time series of the spanwise velocity fluctuation w recorded at several stations along the upper surface of the airfoil. We observe a shift in the frequency which corresponds to the most energetic motions towards lower values as the recording station moves closer to the trailing edge. This is consistent with the increase of an inertial timescale (ratio of the boundary layer thickness to the edge velocity) as the boundary layer grows under the influence of the adverse pressure gradient. It becomes also evident that the solution has to be sampled over several time units c/U_∞ in order to obtain representative turbulence statistics for the rear part of the airfoil.

3.4.2 Spanwise and time averaged results

Statistics were obtained by averaging the instantaneous flow fields in the spanwise homogeneous direction and in time. Structured mesh data were averaged over $1.1c/U_\infty$, unstructured simulation results over $3c/U_\infty$. Statistics of the structured mesh simulation are not yet fully converged. Figure 2 compares the mean velocity profiles on the upper surface. Both simulations exhibit a small region of mean backflow near the nose. This laminar separation bubble is steady in the structured grid. In the unstructured mesh case, however, the laminar separation is highly unsteady. A laminar shear layer rolls up into vortices at a frequency of $63U_\infty/c$.

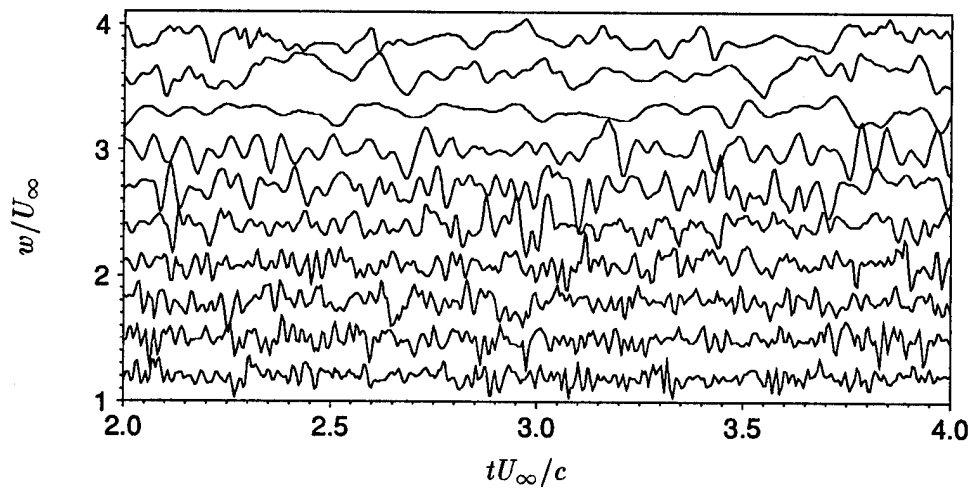

Figure 1: Time series of spanwise velocity fluctuations between stations $x/c = 0.24$ (bottom) and $x/c = 0.98$ (top). The data were taken from the structured mesh simulation close to $y/\delta = 0.04$.

Transition occurs around $x/c = 0.07$ when spanwise variations of the initially purely two-dimensional rollers have been amplified sufficiently. Because of the different nature of transition near the nose in the two simulations, the mean velocity profiles deviate considerably with the unstructured mesh case being less full. Mean flow profiles remain different between both simulations over the entire upper surface. The unstructured mesh case predicts separation and backflow near the trailing edge whereas the flow remains attached in the structured mesh simulation. Consequently, measured and computed pressure distributions deviate considerably for the structured mesh case (Figure 3) and agree better for the unstructured simulation. The structured mesh simulation reaches a higher suction peak than the unstructured case and the measurements. This might be a side effect of filtering the solution near the nose in order to eliminate 2-Δ-waves. A detailed study of the near nose flow is currently under way to clarify this issue.

Significant differences with respect to Reynolds stresses are found between the two simulations. The structured mesh case exhibits higher shear stress $\overline{uv}$ and lower anisotropy u'/v' than the unstructured mesh simulation in the first half of the airfoil, see Figures 4, 5. Shear stress and rms-values u' and v' from the structured mesh are in fairly good agreement with the measurements at stations $x/c = 0.53$ and $x/c = 0.59$. But further downstream, the stresses are much smaller than the measured ones. Conversely, the unstructured mesh simulation tends to overpredict the streamwise rms-value u' in the middle part of the airfoil but is close to measurements in the separated region. The observation of high Reynolds stress anisotropy in conjunction with rather low shear stress values in the FE-case is probably related to the upstream transition mechanism. This underlines the importance of better understanding and definition of the flow near the nose. Realistic agreement with measured data can probably be expected only for a simulation in which its early boundary layer has similar features as the

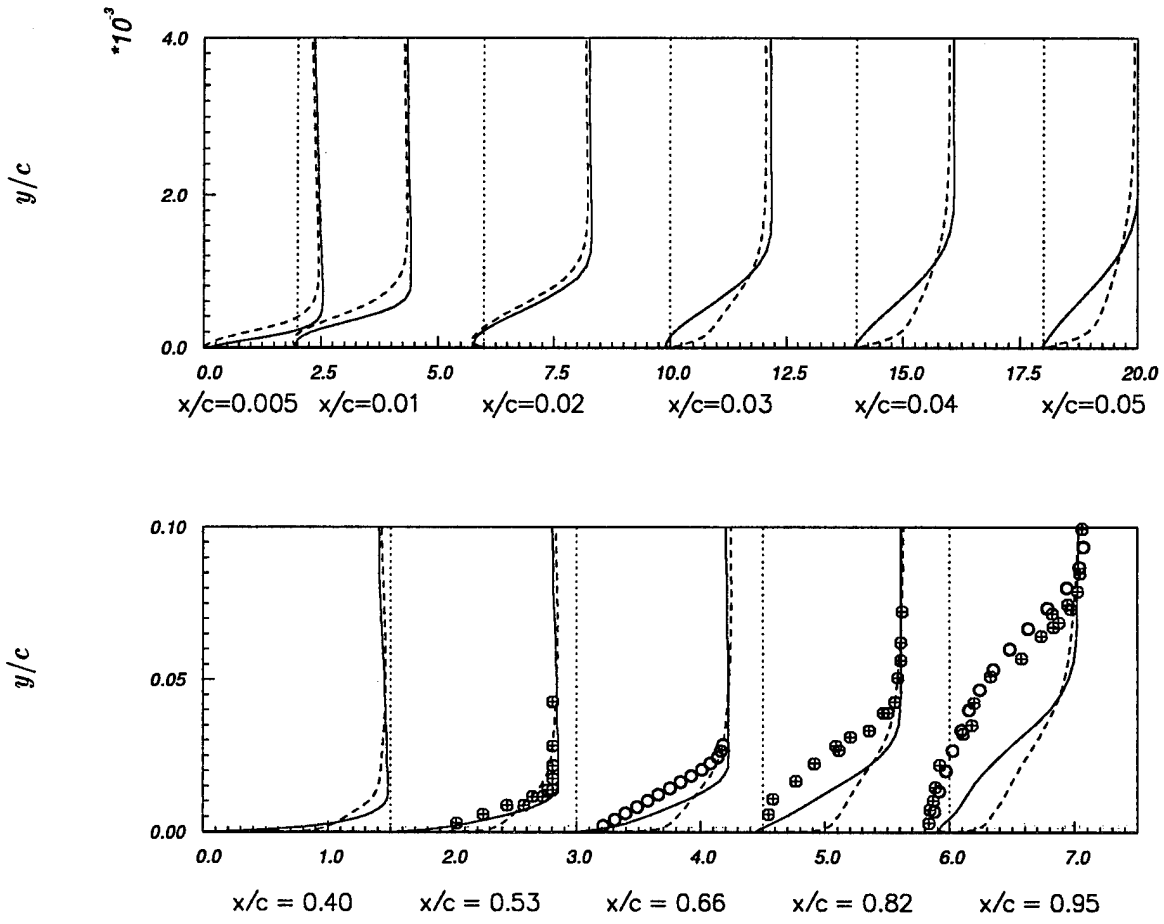

Figure 2: Mean velocity U/U_∞ parallel to the upper surface versus y/δ from FE-simulation ——— , structured mesh ---- , Wadcock $\oplus$, and Hastings $\circ$.

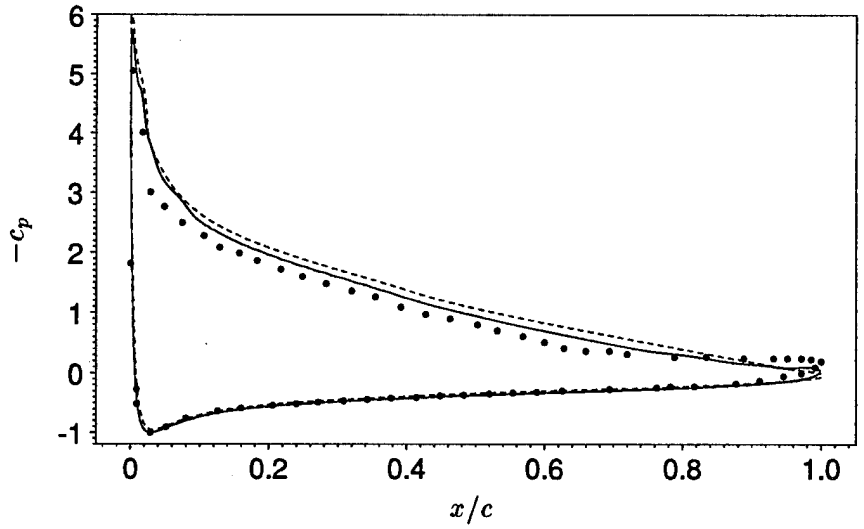

Figure 3: Pressure distribution from Wadcock • , FE-simulation —— , and structured mesh simulation ---- .

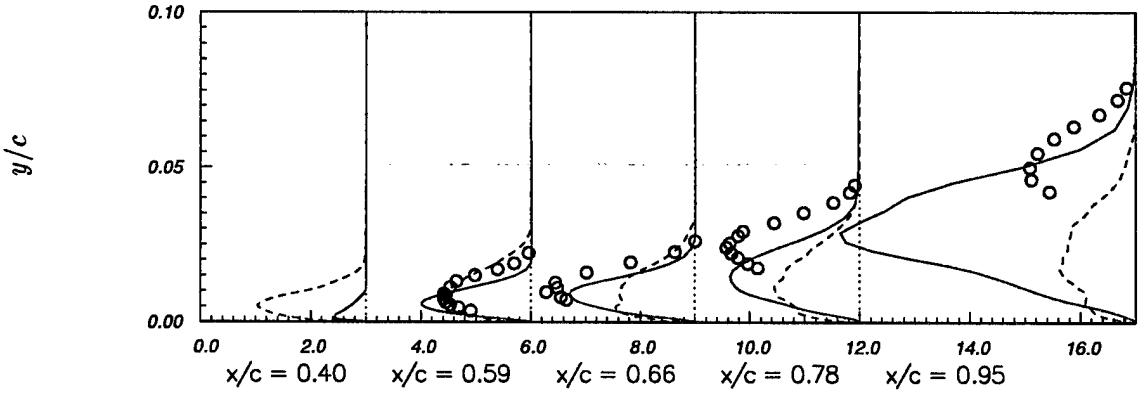

Figure 4: Shear stress $\overline{uv} \times 500$ from Hastings ∘ , FE-simulation —— , and structured mesh simulation ---- .

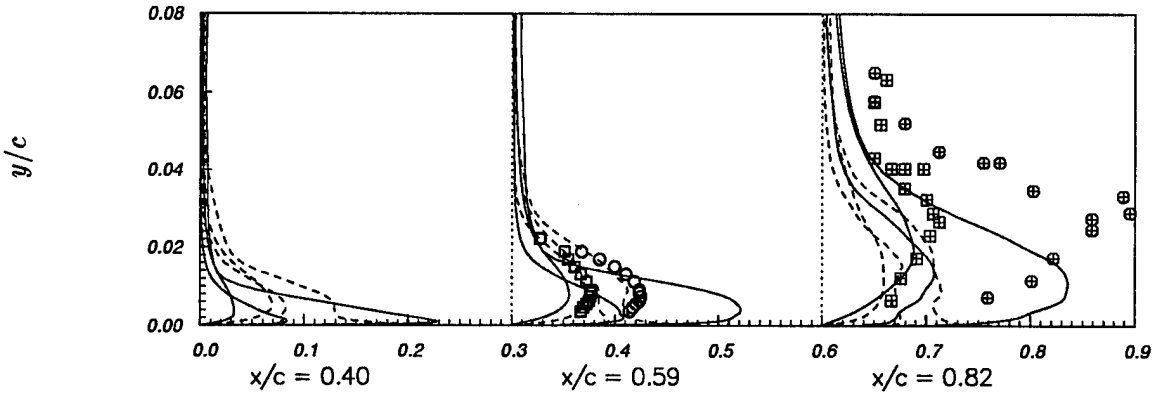

Figure 5: Rms values u', v', w' from FE-simulation —— , structured mesh simulation ---- , and measured u', v' from Hastings o , and Wadcock $\oplus$.

sipation. The subgrid-scale eddy viscosity is about 10-20 times higher than the molecular viscosity in the structured mesh case and about half this value for the unstructured mesh simulation. Because the numerical method for the unstructured mesh provides some damping (stabilization) it can be expected that in this code the subgrid-scale model plays a smaller role compared to a kinetic energy conserving method. Upstream of $x/c = 0.3$ we find that the subgrid-scale stress component τ_{12} contributes between 10 and 15% to the total shear stress.

3.4.3 Integral boundary layer parameters

The only available experimental data for the first half of the airfoil are boundary layer thickness, momentum and displacement thickness. Figures 6, 7 compare these parameters. Despite some scatter in experimental data it seems that the integral boundary-layer parameters of the simulations are in reasonable agreement with the measurements between $x/c = 0.1$ and $x/c = 0.3$. The structured mesh simulation, for which transition occured at $x/c = 0.02$, has a slightly thicker boundary layer than the experiments. The absolute values of θ and δ^* measured by Hastings and Wadcock close to $x/c = 0.2$ are quite different, the shape factor, however, is very similar. Because both experiments predict similar amounts of separation near the trailing edge, it seems that the flow is not very sensitive with respect to the boundary layer thickness near the airfoil nose. Comparing Hastings' with Wadcock's data we observe that Hastings whose boundary layer was thicker near the nose predicts separation slightly earlier than Wadcock. In the simulations this trend is reversed: the structured simulation with the initially thicker boundary layer predicts less backflow near the trailing edge compared to the FE-simulation which started from an initially thinner boundary layer.

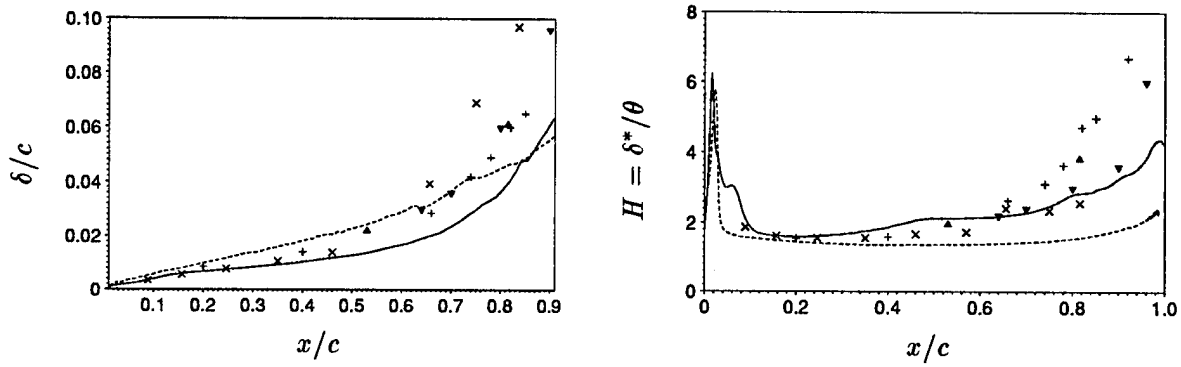

Figure 6: Boundary layer thickness δ_{995} and shape factor along the upper surface of the airfoil. Symbols: —— FE-simulation, ---- structured mesh simulation, × Wadcock (Pitot tube), + Hastings, ▲ Wadcock (rake), ▽ Coles.

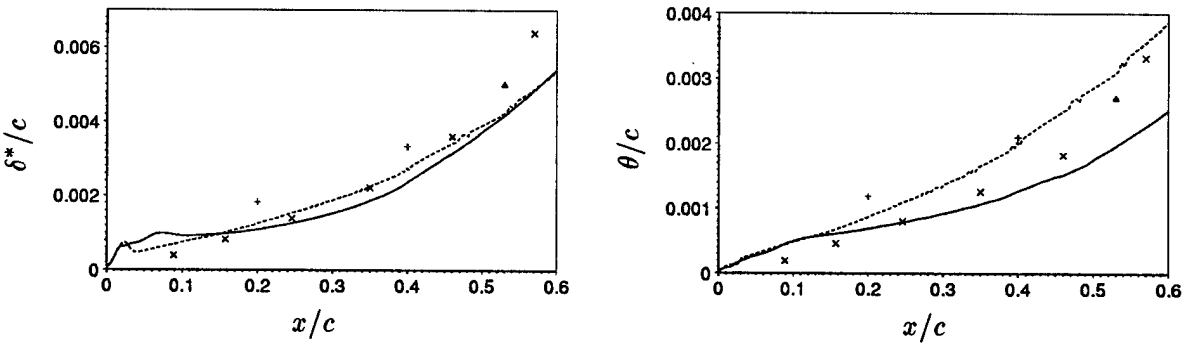

Figure 7: Displacement thickness δ^* and momentum thickness θ along the upper surface. Symbols as in previous figure.

3.4.4 Two-point correlations

Spanwise two-point correlations were computed from 20 instantaneous flow fields for several streamwise locations inside of the boundary layer. From the structured mesh simulation we draw some conclusions by monitoring the location of zero-crossing as an indicator of the average spanwise spacing or size of flow structures. This zero-crossing occurs within 2-3 spanwise grid points for all near-wall locations upstream of $x/c = 0.5$. Consistently, an examination of instantaneous flow fields reveals a very streaky structure in the inner part of the boundary layer with typical spacings of the order of a few mesh cells (Figure 9). This indicates that the structured mesh simulation has marginal resolution near the wall. The zero-crossing increases with distance from the wall as a consequence of the changing eddy-structure in the boundary layer. The spanwise resolution is adequate for the outer part of the boundary layer. Towards the rear part of the airfoil we find that the two-point correlations no longer decay to zero. This indicates either that the spanwise extent of the domain is too small or that owing to separation the structures are very coherent near the trailing edge. Variance spectra in the inner layer are flat (close to k^{-1}) near the cutoff wavenumber. In the outer layer they decay like k^{-4}.

3.4.5 Instantaneous flow fields

Figure 8 shows planes normal to the mean flow direction for four different streamwise stations. For the early stations we find that intense streamwise vortices are mainly concentrated near the wall. The intensity of streamwise vortices decreases further downstream. They are no longer concentrated near the wall but appear throughout the whole boundary layer at later stations. Consistent with the finding of intense streamwise vorticity along the first half of the upper surface, we find that the near wall region exhibits streaky structures, Figure 9. Flow structures become larger further downstream where the boundary layer is close to separation. Figure 10 shows a closeup view of the nose section from the FE-simulation.

4 Summary and future plans

The turbulent flow over a NACA 4412 airfoil at angle of incidence corresponding to maximum lift (12°) has been computed via large-eddy simulation. Two different numerical approaches, one based on a conventional structured mesh and one with a more economical unstructured mesh, have been employed. Results from both simulations differ considerably from each other and from the available experimental data. Differences are found with respect to occurrence of transition near the suction peak and with respect to the amount of backflow near the trailing edge. Although both simulations did not attempt to provide a transition mechanism resembling the boundary layer tripping employed in the experiment, the boundary layer characteristics (thickness, shape factor) seem to match the experimental ones at $x/c = 0.1 - 0.2$. Flow development along the upper surface is quite different within both simulations. Whereas the unstructured mesh case predicts a strong thickening of the boundary layer and mean backflow near the trailing edge, the flow remains attached in the structured mesh simulation. The

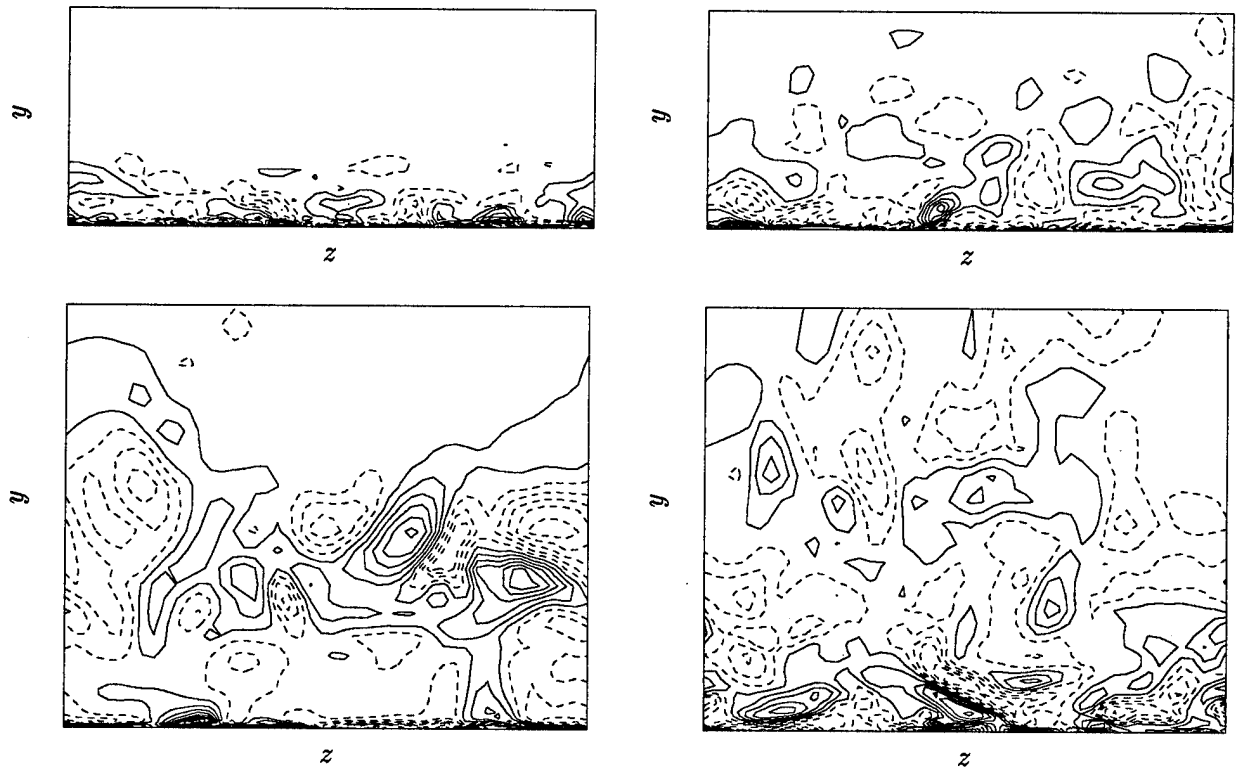

Figure 8: Streamwise vorticity components in planes normal to the mean flow at $x/c = 0.2$ (top left), $x/c = 0.53$ (top right), $x/c = 0.84, 0.95$ (bottom) from the strucutured mesh simulation. The isoline increment of the two lower figures is half that of the two upper figures.

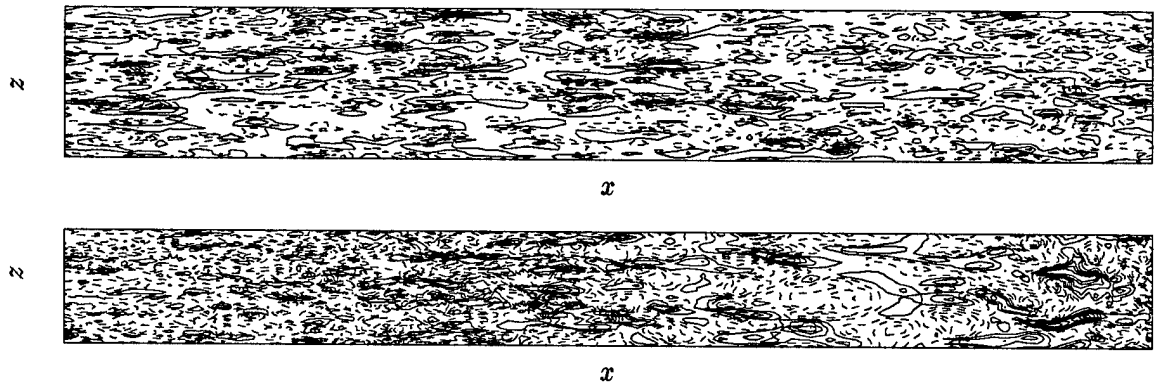

Figure 9: Instantaneous wall-normal velocity component at $y/\delta = 0.03$ from the strucutured mesh simulation between $x/c = 0.24$ and $x/c = 0.59$ (upper figure) and between $x/c = 0.5$ and $x/c = 0.96$ (lower figure).

reason for the different behaviors has not yet been fully understood. Both methods provide similar resolution inside the boundary layer and have similar truncation errors of $O(\Delta x^2)$. A major difference between the methods appears to be the conservation properties with respect to kinetic energy. The structured mesh code is close to conserving energy but suffers from problems which were probably associated with high Reynolds number, boundary conditions, and mesh stretching. The unstructured mesh code on the other hand has an inherent stabilization which guarantees smooth solutions whithout grid-to-grid oscillations. Examination of spectra does not reveal excessive damping of small-scale turbulence in this code. We have performed simulations on coarser meshes with both codes. The results have definitely improved when finer meshes were used. More grid refinement studies are probably needed to determine whether the resolution is adequate.

Our goal for the future is to identify more clearly the cause for the mismatch of the two simulation methods as well as to try to match better the experimental data. Specific issues which we want to target in our future work are:

- How sensitive is the overall flow towards details of flow in the nose section? What role does the transition mechanism play? Is the unsteady laminar separation which was found in the unstructured case a grid-independent result? What resolution in the nose section is required for the structured mesh code to reproduce the laminar, unsteady separation?
- What is the role of numerical damping in the context of large-eddy simulation? Is it possible to prevent the emergence of 2-Δ-waves in the structured mesh case without damaging the evolution of turbulence?
- How sensitive are the results with respect to the angle of attack? Are there possible side-effects (windtunnel walls etc.) in the experiment which affect separation and which cannot be reproduced by the simulations?
- Are the simulations affected by a limited spanwise domain size?
- Is the near-wall resolution sufficient? Do we obtain the same result on an even finer mesh?

Acknowledgments

Computer time for the structured mesh computations was provided through NAS and for the FE-computations through the AFSOR at the AHPCRC in Minnesota. We thank W. M. Chan from NASA Ames for providing the hyperbolic grid generator.

References

Cain, A.B. & Bush, R.H. 1994, Numerical wave propagation analysis for stretched grids. AIAA-94-0172, 32nd Aerospace sciences meeting, Jan 10-13, 1994/Reno, NV.

Chan, W.M., 1993, User's Manual for the HYPGEN hyperbolic grid generator. NASA Technical Memorandum 108791.

Choi, H., Moin, P. & Kim, J. 1993, Direct numerical simulation of turbulent flow over riblets. *J. Fluid Mech.***255**, pp. 503-539.

Choi, H. 1993, Towards large-eddy simulation of turbulent flow over an airfoil. CTR Annual Research Briefs 1993, p. 145.

Coles, D. & Wadcock, A.J. 1979, Flying-hot-wire study of two-dimensional mean flow past a NACA 4412 airfoil at maximum lift. *AIAA Journal*, **17**.

Durbin, P. 1993, Turbulence modeling for non-equilibrium flows. CTR Annual Research Briefs 1993, p. 67.

Germano, M., Piomelli, U., Moin, P. & Cabot, W. H. 1991, A dynamic subgrid-scale eddy viscosity model, *Phys. Fluids A*,**3**, pp. 1760-1765.

Ghosal, S., Lund, T., Moin, P. & Akselvoll, K. 1995, A dynamic localization model for large-eddy simulation of turbulenct flows. *J. Fluid Mech.*, **286**, pp. 229-255.

Hastings, R.C. & Williams, B.R. 1984, Studies of the flow field near an NACA 4412 aerofoil at nearly maximum lift. Royal Aircraft Establishment, Technical Memorandum Aero 2026.

Hastings, R.C. & Williams, B.R. 1987, Studies of the flow field near an NACA 4412 aerofoil at nearly maximum lift. *Aeronautical Journal*, **91**, pp. 29-44.

Jansen, K., Z. Johan, & T.J.R. Hughes 1993, *Comp. Meth. Appl. Mech. Eng.*, **105**, pp.405-433.

Moin, P., Squires, C., Cabot, W., Lee, S. 1991, A dynamic subgrid-scale model for compressible turbulence and scalar transport. *Phys. Fluids A*, **3**,pp. 2746-2757.

Rogers, S.E., Wiltberger, N.L. & Kwak, D. 1992, Efficient simulation of incompressible viscous flow over single and multi-element airfoils. *AIAA-92-0405*, 30th Aerospace sciences meeting, Jan. 6-9, 1992/Reno, NV.

Wadcock, A.J. 1987, Investigation of low-speed turbulent separated flow around airfoils. NASA contractor report 177450.

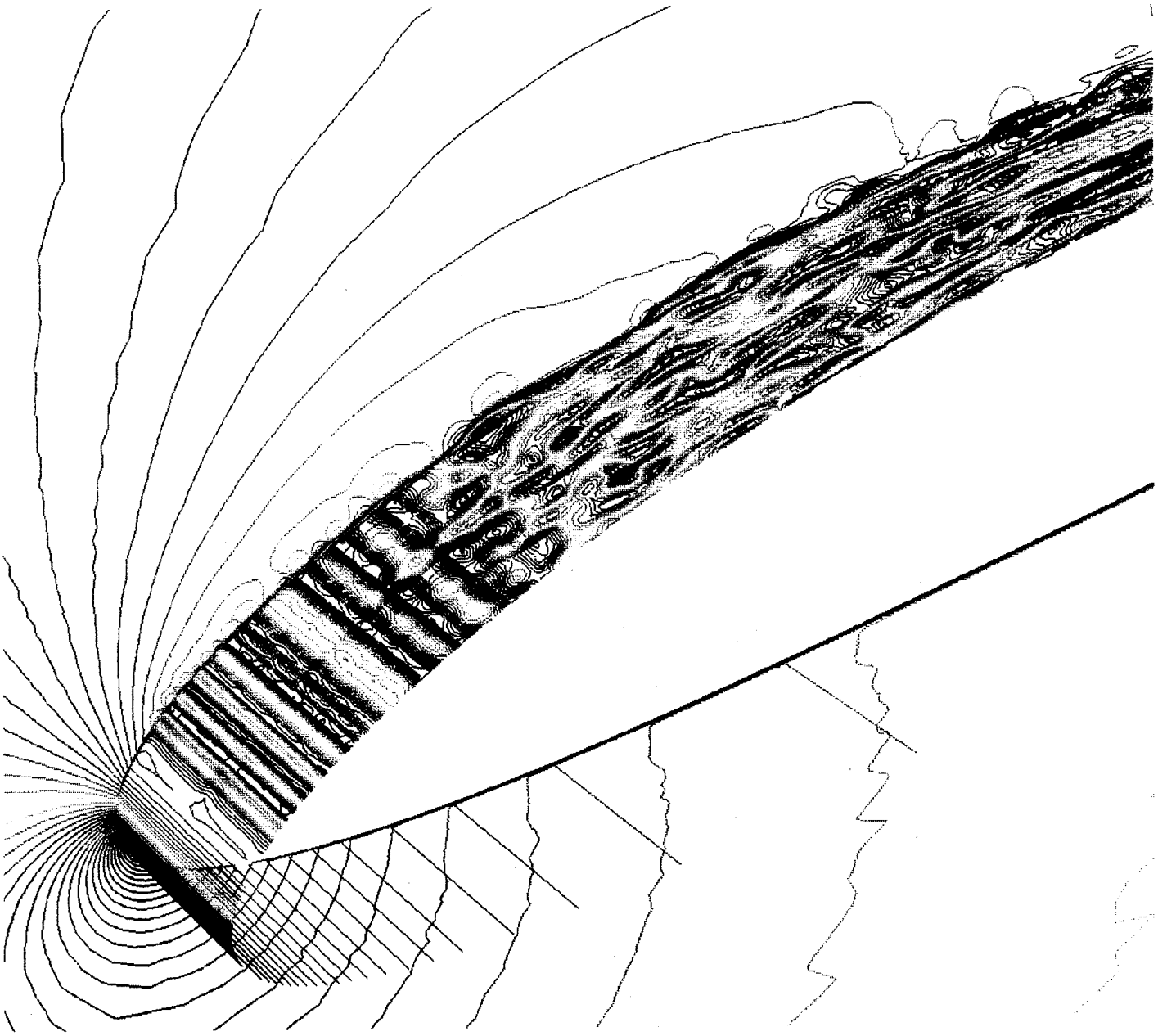

Figure 10. Instantaneous visualization of the streamwise velocity contours from the unstructured-grid simulation (dark blue is negative, green is low speed, red is high speed). Two planes are shown here; a plane parallel to the body (10 points away from the body) and a plane perpendicular to the body. Note the laminar freestream flow stagnates on the nose and is then accelerated around the nose up to the suction peak. After the suction peak the pressure gradient is adverse and the boundary layer separates creating traveling spanwise coherent vortices. Eventually these vortices grow large enough to transition to full three-dimensional turbulence (right 2/3 of the figure).